International Journal of Multiphysics
Volume 18, No. 2, 2024
ISSN: 1750-9548

Calculation of Vibration Characteristics of Water Transport Elbow based on Fluid-structure Interaction

Yue Cui[1], Simin Zhu[2], Nan Lin[3], Huiqing Lan[2,4*], Kexin Tan[5], Xiangbin Yang[1]

[1] Key Lab of Intelligent Equipment Digital Design and Process Simulation, Tangshan University, Tangshan 063000, China

[2] Key Laboratory of Vehicle Advanced Manufacturing, Measuring and Control Technology (Ministry of Education), Beijing Jiaotong University, Beijing 10004, China

[3] China Special Equipment Inspection and Research Institute, Beijing 100029, China

[4] Tangshan Research Institute of Beijing Jiaotong University, Tangshan 063000, China

[5]China University of Petroleum (Beijing), Beijing 102249, China

*Corresponding author.

Abstract

The fluid-structure interaction (FSI) in transportation pipelines directly affects the characteristics of the pipe, primarily causing pipeline vibration. The FSI computational model of a water transport elbow impacted by the fluctuating pressure was established, considering the pressure amplitude and frequency of pulsating fluids, as well as the wall thickness to diameter ratio. Force and modal analyses were conducted using ANSYS Workbench software. Results show that the maximum deformation occurs in the middle of the bending section. The natural frequency of the elbow is significantly reduced under FSI, with the sixth natural frequency reduced by 35.9% to 610.48 Hz. As the excitation frequency increases, the displacement and acceleration response of the monitoring point exhibit peaks at the second and fifth natural frequencies, respectively. To minimize the impact of resonance on the lifespan of pipelines, elbows with large bending-to-diameter ratio should be used for low-frequency vibration conditions, whereas bent pipes with small bending-to-diameter ratio should be used for high-frequency vibration conditions. This approach simultaneously increases the wall thickness at the pipeline connections.

Keywords: Fluid-Structure Interaction Computational Model (FSICM), Fluctuating Pressure(FP), Mode Superposition(MS), Natural Frequency(NF), Harmonic Analysis(HA)

1. Introduction

Liquid transport pipelines have an extensive use in various industries, such as petrochemicals, energy and power industries, shipbuilding, and marine engineering. Unsteady flow fluids often cause significant vibration in the pipeline owing to the presence of a large number of branch pipelines and fluid pulsation excitation caused by water pumps in the pipeline system. The noise generated by the pipeline system is not simply caused by pipeline vibration or fluid flow inside the pipeline, but by the coupling between the pipeline structure and the fluid inside the pipeline. Therefore, vibration noise and flow noise coexist and affect each other. The interaction between fluid and structure caused by structural field and flow field deformation is studied through computational analysis to guarantee safe and stable operation of pipeline systems.

Numerous studies by domestic and foreign scholars have shown that fluid pulsation pressure in flow pipelines is the main cause of pipeline vibration. Dou et al.[1] developed an user-defined function UDF control file in Fluent, setting the inlet flow velocity of the pipeline as a pulsating form. They also analyzed the influence of different fluid pulsation frequencies on pipeline amplitude under the condition of flow velocity pulsation. Xia et al.[2]

found that unsteady fluid excitation can cause vibration in hydraulic pipelines. Under the excitation of pulsating fluid, the displacement curve of monitoring points continuously decays, and eventually a small amplitude vibration occurs at the equilibrium position of the pipeline. In the analysis of single-path and double-path FSI, Yu et al.[3] considered the influence of pulsating pressure and found that the maximum deformation of the pipe under double-path FSI are greater than those under single-path FSI. Xiao et al.[4] focused on the structural vibration caused by fluid excitation inside the pipe. They analyzed the effect of flow velocity on the structural vibration characteristics by introducing additional mass under single-path FSI and obtained the additional mass and natural frequency of the pipeline structure. Zhu et al. [5] used pseudo-excitation method for solving vibration responses and found that the walled theory differ in wave transmission. Zhao et al.[6] studied the influence of the clamping force on the frequency characteristics of air- and liquid-filled pipelines under experimental control. Yu et al.[7] conducted modal analysis on typical pipelines and found that setting ideal boundaries would lead to differences in vibration analysis between simulation and experimental results. Keramat et al.[8] analyzed the effect of viscoelastic water hammer on pipelines under FSI. Bao et al.[9] considered the internal and external flow factors of the pipeline, as well as the influence of axial force on the pipeline section, and then analyzed the inherent characteristics of submarine-suspended flow pipelines. Gao et al.[10] described the nonlinear FSI dynamics of pipes with the linear partial differential model. The results reveal the resonant laws of aircraft hydraulic pipes under complex constraints. Yang et al.[11] analyzed the influence of material parameters on the vibration of the pipe based on the characteristic line method. Lin et al.[12] investigated the effect of fluid on the vibration characteristics of hydraulic pipeline systems when passing through pipeline attachments. Zhao et al.[13] studied the flow-induced vibration mechanism of elbow and conducted numerical simulation to obtain the main location of pipe excitation force. Quan et al. [14] solved the the FSI vibration by using frequency-domain transfer method to analyze the axial vibration of the pipeline.

The double-path FSI method is used to simulate the deformation of the pipe wall. By analyzing the influence of different structural parameters of pipelines on the natural frequency of pipeline vibration, aim to solve the problem of the fluid excitation inside the pipe on the structural vibration characteristics.

2. Calculation Method

2.1 FSI dynamic equation

The fluid flow rate in the pipeline is constantly changing over time, generating periodic pressure waves in the pipeline. The pressure pulsation generated by flow pulsation causes FSI vibration inside the pipeline, resulting in vibration noise. The FSI vibration equation under pulsating fluid excitation provides the dynamic characteristics of axial, transverse, and torsional vibrations of flow pipelines; the equation solved through computer double-path FSI simultaneous solution is expressed as follows:

Torsion equation of pipeline:

$$\frac{\partial m_z}{\partial z} + \rho_p J \frac{\partial \dot{\theta}_z}{\partial t} = 0 \tag{1}$$

The bending motion equation of pipeline in the y-z plane:

$$\frac{\partial \dot{w}_y}{\partial z} + \dot{\theta}_x + \frac{1}{\kappa G A_p} \frac{\partial f_y}{\partial t} = 0 \tag{2}$$

$$\frac{\partial \dot{\theta}_x}{\partial z} + \frac{1}{EI_p} \frac{\partial m_x}{\partial t} = 0 \tag{3}$$

$$\frac{\partial f_y}{\partial z} + \left(\rho_f A_f + \rho_p A_p\right) \frac{\partial \dot{w}_y}{\partial t} = 0 \tag{4}$$

$$\frac{\partial m_x}{\partial z} - f_y + \left(\rho_f I_f + \rho_p I_p\right)\frac{\partial \dot{\theta}_x}{\partial t} = 0 \tag{5}$$

The bending motion equation of pipeline in the x-z plane:

$$\frac{\partial \dot{w}_x}{\partial z} - \dot{\theta}_y + \frac{1}{\kappa G A_p}\frac{\partial f_x}{\partial t} = 0 \tag{6}$$

$$\frac{\partial \dot{\theta}_y}{\partial t} + \frac{1}{EI_p}\frac{\partial m_y}{\partial t} = 0 \tag{7}$$

$$\frac{\partial f_x}{\partial z} + \left(\rho_f A_f + \rho_p A_p\right)\frac{\partial \dot{w}_x}{\partial t} = 0 \tag{8}$$

$$\frac{\partial m_y}{\partial z} + f_x + \left(\rho_f I_f + \rho_p I_p\right)\frac{\partial \dot{\theta}_y}{\partial t} = 0 \tag{9}$$

The axial motion equation of pipeline:

$$\frac{\partial f_z}{\partial z} + \rho_p A_p \frac{\partial \dot{w}_z}{\partial t} = 0 \tag{10}$$

$$\frac{\partial P}{\partial z} + \rho_f \frac{\partial V}{\partial t} = 0 \tag{11}$$

$$\frac{\partial \dot{w}_z}{\partial z} + \frac{1}{EA_p}\frac{\partial f_z}{\partial t} + \frac{\mu R}{\delta E}\frac{2R-\delta}{2R+\delta}\frac{\partial P}{\partial t} = 0 \tag{12}$$

$$\left[\frac{1}{K_f} + \frac{2}{E}\left(\frac{R}{\delta} + \frac{2R}{2R+\delta}\mu\right)\right]\frac{\partial P}{\partial t} + \frac{2\mu}{EA_p}\frac{\partial f_z}{\partial t} + \frac{\partial V}{\partial z} = 0 \tag{13}$$

where m_x, m_y, and m_z are the bending moments of the pipeline around the x, y, and z coordinate axes, respectively; $\dot{w}_x$, $\dot{w}_y$, and $\dot{w}_z$ are the velocities of the pipeline along the *x*, *y*, and *z* directions, respectively; $\dot{\theta}_x$, $\dot{\theta}_y$, and $\dot{\theta}_z$ are the rotational speeds of the pipeline around the *x*, *y*, and *z* directions, respectively; ρ_p is the density of the pipeline; ρ_f is the average density of the fluid inside the pipeline; *J* is the polar inertia of the pipeline section; I_p is the moment of inertia of the pipeline section; I_f is the moment of inertia of the fluid cross-section; f_x, f_y, and f_z are the internal forces of the pipeline wall along the x, y, and z directions, respectively; E is the elastic modulus of the pipeline material; G is the shear modulus of the pipeline; μ is the Poisson's ratio; A_p is the cross-sectional area of the pipeline; κ is the shear correction coefficient of the pipeline; P is the fluid pressure; V is the average velocity of the fluid across the entire cross-section; R is the radius of the pipeline; δ is the wall thickness of the pipeline.

2.2 Calculation Model of Pipeline

An elbow in the ship's water supply pipeline system was selected to establish a double-path FSI model. Data transmission was bidirectional in the double-path FSI calculation. The analysis results of the fluid were transmitted to the pipeline through the FSI surface, and those of the pipeline are then transmitted to the fluid analysis. After several cyclic iterations and step converges, the solution of the coupling field over the entire time history can be obtained. This approach ultimately achieves the solution of the pipeline vibration process[15]. The

flow pipeline model is shown in Figure. 1, illustrating that both ends of the pipeline are fixed and horizontally placed, and the interior of the pipeline is a fluid domain.

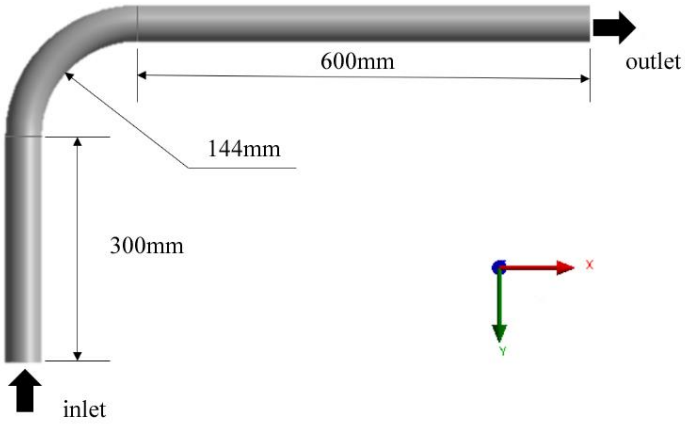

Figure 1 Elbow model

The pipeline adopts structured grid division, with a grid size of 0.5 mm and a grid count of 1.85×10^5. The expansion layer was set on the pipeline inner wall, the remaining fluid region was divided into tetrahedral grids, and the number of fluid area grids is 7.56×10^5. The $k-\varepsilon$ turbulence model was used to solve the flow field region, and a dynamic mesh was set at the boundary between the fluid and the pipe wall for accurate solution. The boundary conditions for flow field calculation are velocity inlet and pressure outlet, and the convergence accuracy of the solution is 1×10^6. The pipeline structural parameters is shown in Table 1.

Table 1 Pipeline structure parameters

E ($\mathrm{N\cdot m^{-2}}$)	ρ ($\mathrm{kg\cdot m^{-3}}$)	μ	δ 10^{-3}/m	d $\mathrm{m^{-3}}$/m
2×10^{11}	7850	0.3	4	40

3. Simulation Analysis

The flow pulsation generated by fluid motion is the excitation source of pipeline vibration in the FSI vibration analysis. Therefore, the pulsating pressure, frequency, and velocity of the fluid were considered the research objects to analyze their impact on pipeline vibration.

In the analysis, the fluid inside the pipeline is assumed to be water at 25 ℃. The flow pulsation at the inlet of the pipeline is set with a flow rate of 10 m3/h and a flow pulsation frequency of 50 Hz. The simulated speed at the inlet of the pipeline was $V=2.21\times\left[1+0.05\sin\left(100\pi t\right)\right]$, and the working pressure is 1 MPa.

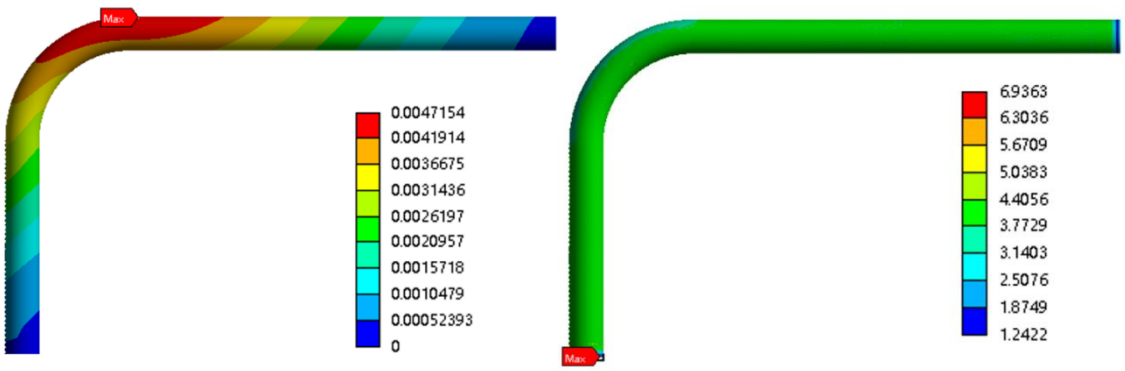

(a)Deformation of pipeline (mm) (b) Mises stress of pipeline (MPa)

Figure 2 Deformation and Mises stress of pipeline

In Figure. 2(a), the maximum deformation of the elbow occurred in the middle of the pipeline because the flow direction of the pulsating fluid changed at the corner. Thus, additional forces on the pipe wall are generated, thereby increasing the pipeline deformation. In Figure. 2(b), the maximum stress occurred near the inlet of the elbow because of the pipeline deformation caused by the pressure impact of pulsating fluid. The fixed constraints at both ends of the pipeline result in significant stress near the inlet.

Under the same initial conditions, the vibration response of the elbow at different pulsating pressure amplitudes (1, 2, 3, and 4 MPa) and pulsating frequencies (50, 100, 150, and 200 Hz) is calculated, and the calculation results are shown in Figure.3. The vibration acceleration of the pipeline elbow increased with the increase in pressure amplitude and pulsation frequency. The impact of pulsation frequency on the vibration acceleration of the elbow was greater than that of pressure amplitude. The vibration acceleration reached the extreme value of 1600 mm/s^2 at a pulsating frequency of 200 Hz and pressure amplitude of 4 MPa.

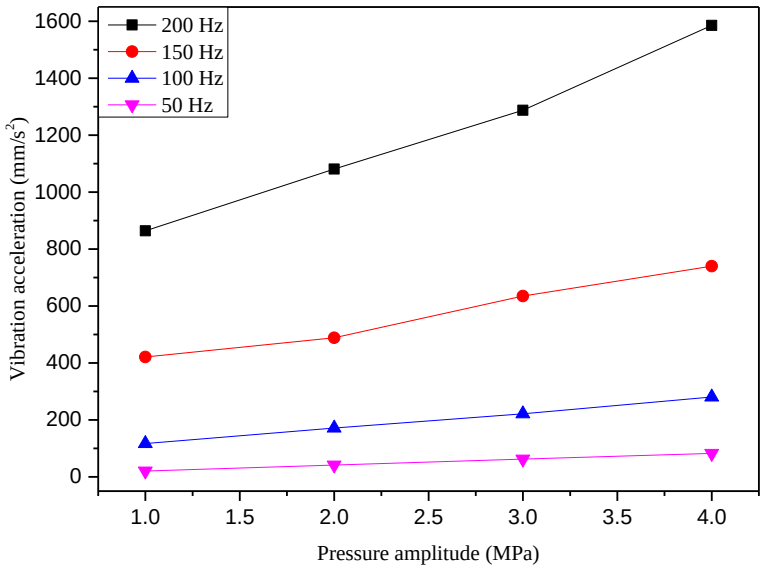

Figure 3 Vibration acceleration change curve of elbow measuring point

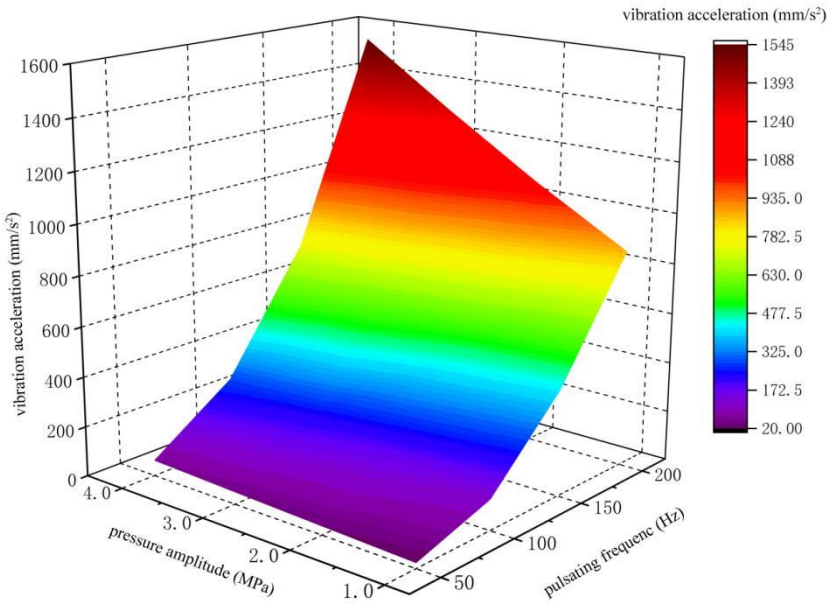

Figure 4 Response of vibration acceleration of elbow to the amplitude and frequency of pulsating pressure

Figure 4 illustrates that the orthogonal experimental method was used to evenly divide the pressure (1–4 MPa) and pulsation frequency (50–200 Hz) within the range of values. In addition, double-path FSI vibration analysis of the pipeline was conducted for each combination of pressure and pulsation frequency. The impact of pulsation frequency on the vibration acceleration of elbow was greater than that of pressure amplitude. When the pulsation frequency avoids resonance zone, the fluid pulsation frequency can be effectively reduced by adjusting the input power source in the pipeline system, thereby reducing the vibration.

4. Result Analysis

In the study of pipeline vibration characteristics, the natural frequencies of the pipeline were calculated separately, that is, considering and ignoring the FSI effect.

Table 2 Comparison among natural frequencies for the elbow

Modal order	Not considering FSI (Hz)	Considering FSI (Hz)	Relative error
1	176.20	155.28	11.9%
2	421.05	372.85	11.9%
3	486.98	430.07	11.7%
4	943.35	610.48	35.3%
5	976.79	843.57	13.9%
6	1359.90	871.84	35.9%

Table 2 shows that considering the FSI between the pipeline and the fluid remarkably affected the natural frequency of the pipeline. When considering the influence of FSI, the frequency corresponding to each order of the pipeline was significantly lower than when ignoring the FSI effect. Moreover, the maximum decrease in natural frequency occurred in the fourth and sixth orders of the pipeline, exceeding 35%. When considering FSI, the mass of the fluid was attached to the pipeline, increasing the inertial force of the entire pipeline system and reducing the natural frequency.

4.1 Effects of different structural parameters on pipeline vibration characteristics

Figure.5 shows that under the same initial conditions, the pipeline wall thickness was changed to 2, 3, 5, and 6 mm, respectively.

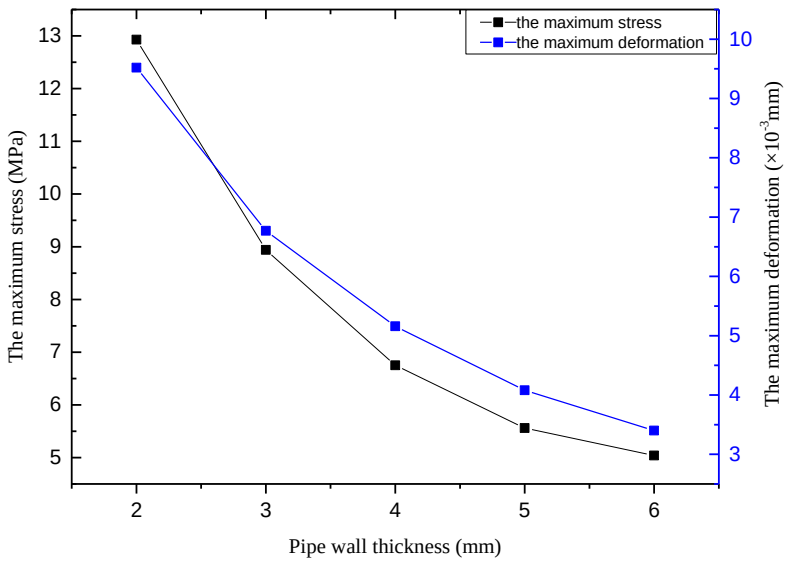

Figure 5 Influence of wall thickness variation on the maximum stress and deformation of elbow

As the wall thickness increases, the maximum Mises stress and maximum deformation decrease accordingly. When the wall thickness of the pipe was 6 mm, the maximum stress of the elbow decreased to a minimum value of 5 MPa, and the deformation of the pipeline decreased to 3.4×10-3 mm.

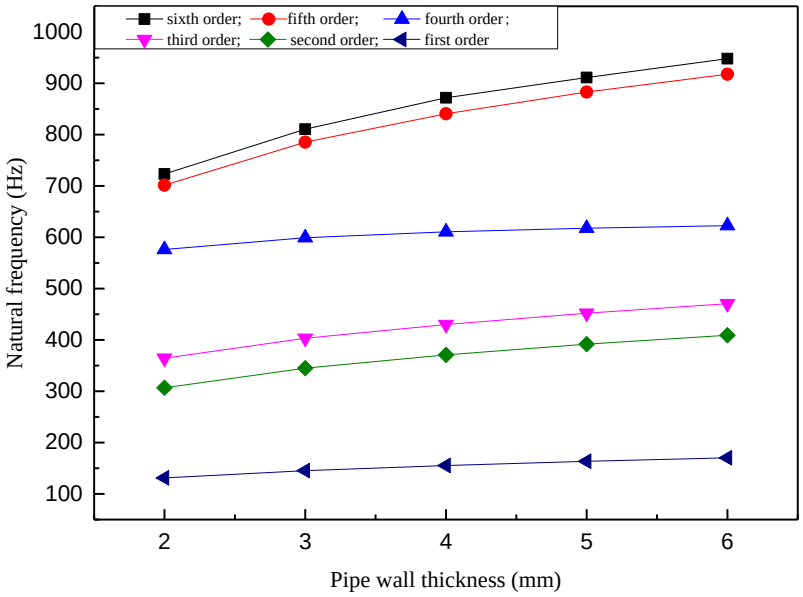

Figure 6 Natural frequency that varies with wall thickness

The natural frequencies of the elbow with wall thickness is shown in Figure. 6. When the wall thickness increased to 6 mm, the first natural frequency increased by 30.0% compared with that when the wall thickness was 2 mm, reaching 910 Hz. The increase in wall thickness improved the overall stiffness of the pipeline, thereby enhancing the natural frequency of the pipe.

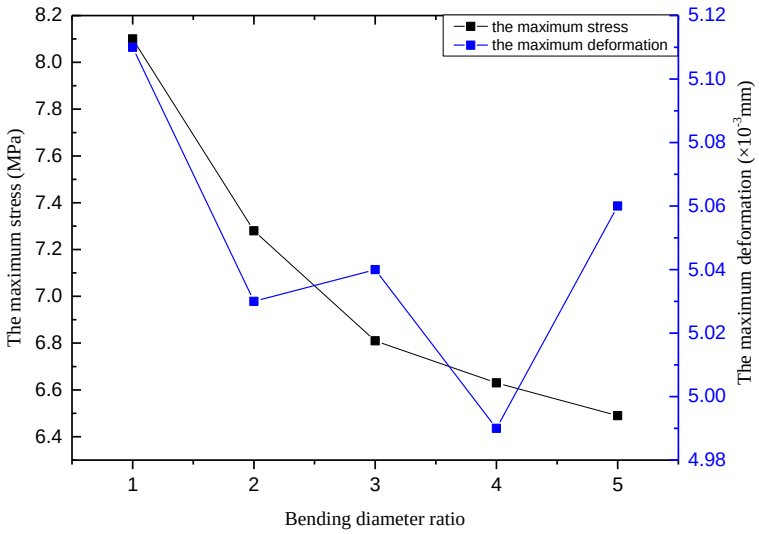

Figure 7 Influence of bending diameter ratio on the equivalent stress and maximum deformation of elbows

Figure 7 shows that under the same initial conditions, when the bending diameter ratio was changed, the bending radius corresponded to 48, 96, 144, 192, and 240 mm. The calculation showed that the bending diameter ratio had a significant impact on the maximum equivalent stress. The findings exhibited a decreasing trend as the pipe

bending radius increased. The maximum equivalent stress decreased as the bending radius of the elbow increased, reaching a minimum value of 6.5 MPa at a bending radius ratio of 5.

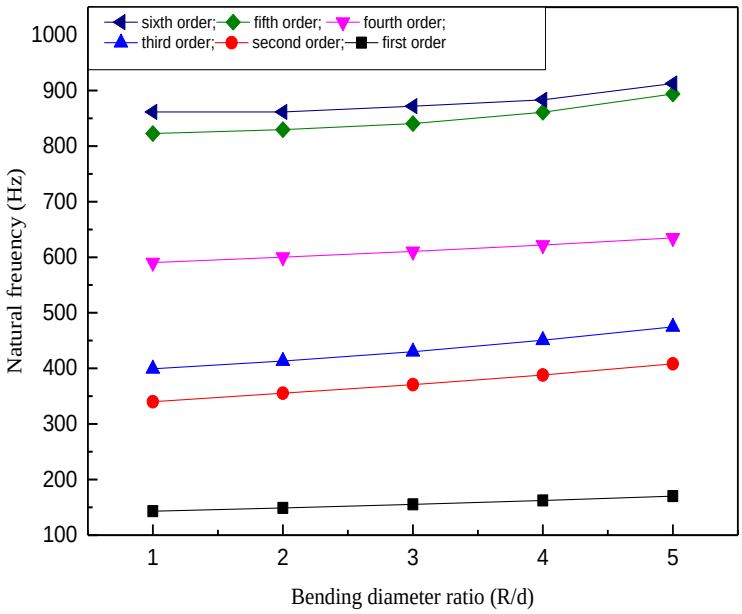

Figure 8 Change in natural frequency with bending diameter ratio

The variation of the first six natural frequencies of the elbow with different bending diameter ratios is shown in Figure 8. The first to third natural frequencies of the elbow increased significantly with the increase in the pipe diameter ratio. And the fifth and sixth orders did not increase significantly when the bending diameter ratio was small. The fourth natural frequency showed a slower growth trend as the bending diameter ratio increased.

4.2 Harmonic response analysis

The modal superposition method was used to perform harmonic response analysis on the elbow based on the modal analysis results of FSI. When conducting harmonic response analysis on the elbow, the excitation amplitude is set to 1 MPa and the pipeline excitation frequency range from 100 Hz to 1000 Hz. The outer wall of the curved part of the pipeline was selected as the key monitoring location, and the response relationship among the displacement, acceleration, stress, and the excitation frequency was analyzed.

As shown in Figure. 9, with the increase in excitation frequency, the displacement and acceleration of the bending part of the elbow showed peaks near the second natural frequency (approximately 370 Hz) and the fifth natural frequency (approximately 840 Hz).

The displacement and acceleration responses in the z direction were much smaller than those in the two other directions, owing to fixed constraints at the inlet and outlet of the pipeline and the excitation mainly coming from the x and y directions. Figure. 9(a) illustrates that when the excitation frequency was 370 Hz, the displacement peaks in the x and y directions reached 3.27×10^{-2} and 5.23×10^{-2}mm, respectively. When the excitation frequency was 840 Hz, the displacement peaks in the x and y directions reached 0.19 and 0.15 mm, respectively. Figure. 9(b) shows that the acceleration response trend was similar to that of displacement response. When the excitation frequency was 370 Hz, the peak acceleration in the x and y directions reached 1.77×10^{5} and 2.82×10^{5} mm/s^2, respectively. When the excitation frequency was 840 Hz, the peak acceleration in the x and y directions reached 5.42×10^{5} and 4.27×10^{5} mm/s^2, respectively. In the pipeline system design and structural optimization, constraints can be placed on the x and y directions of the elbow to reduce vibration.

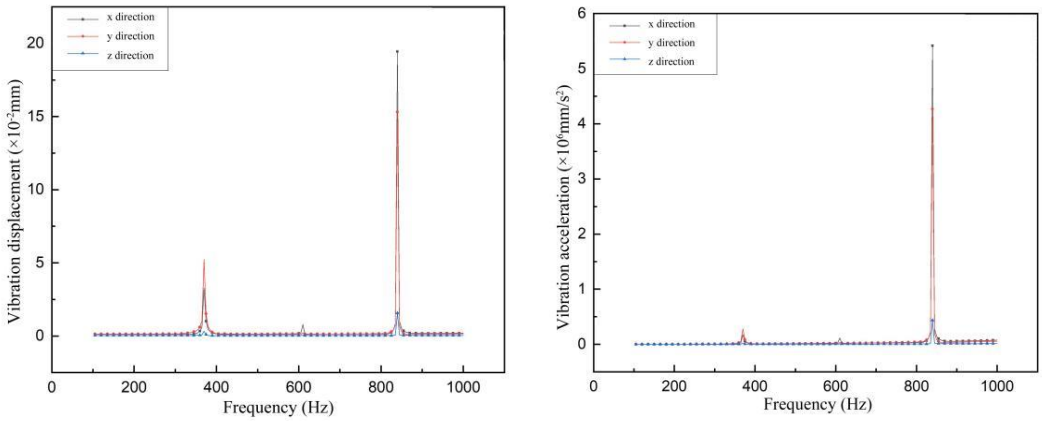

(a)Vibration displacement-frequency response (b) Vibration acceleration-frequency response

Figure 9 Vibration characteristic response curve

5. Conclusions

A FSI model of water transport elbow was built, and the vibration characteristics were analyzed and calculated in a detail.

(1)When pulsating water flowed into the elbow, additional forces were generated on the curved section of the pipe wall, causing deformation. The maximum deformation occurred in the middle of the pipe, and the maximum Mises stress 6.93 MPa appeared at the inlet of the pipe.

(2)The vibration acceleration of the elbow increased with the increase in pressure amplitude and pulsation frequency. The vibration acceleration reached the extreme value of 1600 mm/s^2 at a pulsating frequency of 200 Hz and pressure amplitude of 4 MPa. The impact of pulsation frequency on the vibration acceleration of the elbow was greater than that of pressure amplitude. When the pulsation frequency avoids the resonance zone, the fluid pulsation frequency can be effectively reduced by adjusting the input power source in the pipeline system, thereby reducing the vibration.

(3)As the wall thickness increases, the maximum Mises stress and maximum deformation decrease accordingly. When the wall thickness increased to 6 mm, the first natural frequency increased by 30.0% compared with that when the wall thickness was 2 mm, reaching 910 Hz. Where economically feasible, thick-walled pipes or increased wall thickness at pipe connections can be used to reduce pipeline vibration.

(4)The first to third natural frequencies of the elbow increased significantly with the increase in the pipe diameter ratio. The natural frequencies of the fifth and sixth orders did not increase significantly when the bending diameter ratio was small. The fourth natural frequency showed a slower growth trend as the bending diameter ratio increased. For low-frequency vibration, elbows with a larger bending to diameter ratio should be used, whereas elbows with a smaller bending to diameter ratio should be applied to high-frequency vibration.

(5)With the increase in excitation frequency, the displacement and acceleration of the bending part of the elbow showed peaks near the second and the fifth natural frequency. When the excitation frequency was 840 Hz, the peak acceleration in the x and y directions reached 5.42×10^5 and 4.27×10^5 mm/s^2, respectively.

The calculation of vibration characteristics of water transport elbow based on FSI can improve the lifespan of pipelines to the greatest extent possible.

Acknowledgment

This research was funded by Xiong'an New Area Science and Technology Innovation Project, National Key R&D Program of China (no. 2022XAGG0147); and the Development Funds of the Central Government for Local Science and Technology (no. 236Z1701G).

References

[1] Dou, Y., Yu, K., Yang, X. Finite element analysis of fluid-structure interaction vibration of curved pipe. *Mach. Des. & Manu. Eng.*, 2017, 46(2), pp. 18-21.

[2] Xia, Y., Zhang, C. Hydraulic pipeling fluid-structure interaction vibration calculation based on ANSYS Workbench. *Fl. Pow. Trans. and CTL.*, 2017, 3(82), pp. 41-44.

[3] Yu, S., Ma, L., Yu, L. Analysis of dynamic characteristics of fluid-structure interaction in curved infusion pipelines. *Noi. & Vib. CTL.*, 2015, 35(4), pp. 43-47.

[4] Xiao, B., Zhou, Y., Gao, C. Analysis of vibration characteristics of pipeline with fluid added mass. *J. Vib. and Shock*, 2021, 40(15), pp. 182-188.

[5] Zhu, H.Z., Wu, J.H. A study on the vibration analysis of thick-walled, fluid-conveying pipelines with internal hydrostatic pressure, *Appl. Sci.* 2023, 11(12), pp. 2338-2356.

[6] Zhao, S. Dynamic of aero-engine external piping and fluid-structure interaction analysis. *NUAA.*, 2014.

[7] Yu, S., Lu, T., Wei, G. Research on vibration characteristics of typical pipe. *MATEC Web of Conferences*, 2018, pp. 1-4.

[8] Keramat, A., Tijsseling, A.S., Hou, Q. Fluid-structure interaction with pipe-wall viscoelasticity during water hammer. *J. Fluid Struct.*, 2012, 28(10), pp. 434-455.

[9] Bao, R., Bi, W., Tang, L. Differential-quadrature method to analyze natural characteristics of submarine fluid conveying pipeline. *J. Vib. & Shock*, 2008, 27(11), pp. 73-76.

[10] Gao, H.H., Guo, C.H., Quan L.X. Frequency domain analysis of fluid-structure interaction in aircraft hydraulic pipe with complex constraints, *Processes.* 2022, 10(6), pp. 1161-1184.

[11] Li, J., Wang, K., Yin, Y. Effect of periodic pulsation fluid on vibration characteristics of hydraulic pipe of aircraft. *Mach. Tool and Hydrau.*, 2014, 42(11), pp. 5-8.

[12] Chen, M., Duan, J., Shu, D. Study on influence of fluid parameters on axial coupled vibration of pipeline conveying multiphase flow. *INT J CHEM ENG*, 2017, pp. 1-10.

[13] Xie, C., Wang Z. Fluid-solid coupling numerical simulation of L-pipe vibration induced by gas-liquid two phase internal flow. *CN. Petro. Mach.*, 2019, 47(4), pp.124-128.

[14] Quan, L.X., Che, S.C., Guo, C. H. Axial vibration characteristics of fluid-structure interaction of an aircraft hydraulic pipe based on modified friction coupling model. *Appl. Sci*, 2020, 10(10), pp. 3548-3567.

[15] Li, S. Dynamic analysis of fluid-structure interaction of pipe systems conveying fluid. *HEU*, 2015.